HIGH ACCURACY PRECESSION MEASUREMENT

WITH AN AUTOMETRIC GYRO

by

D. I. Shalloway and D. H. Frisch

CSR TR-70-6   July 1970

CENTER FOR SPACE RESEARCH ⊂SR

MASSACHUSETTS INSTITUTE OF TECHNOLOGY

HIGH ACCURACY PRECESSION MEASUREMENT

WITH AN AUTOMETRIC GYRO

by

D. I. Shalloway and D. H. Frisch

HIGH ACCURACY PRECESSION

MEASUREMENT WITH AN

AUTOMETRIC GYRO[*]

David I. Shalloway and David H. Frisch
Department of Physics and Center for Space Research
Massachusetts Institute of Technology
Cambridge, Massachusetts

ABSTRACT

The mathematical analysis of the signal from an autometric gyro with a linearly ruled reticle is presented and applied to proposed high accuracy precession measurements. The angular measurement accuracy for a practical gyro is limited by random reticle errors to about $\pm\ 4\ \cdot\ 10^{-9}$ radians.

NOMENCLATURE

$a_n(\rho)$ ≡ Fourier coefficients of $I(\theta)$

$a_n^r(\rho)$ ≡ rapidly varying part of $a_n(\rho)$

a_m^x, b_m^x ≡ Fourier coefficients of $I(x)$

$a^\psi(\rho)$, $b^\psi(\rho)$ ≡ Fourier sine and cosine transforms of $\psi_x(x)$

α ≡ angle between star and gyro spin axis

α_o ≡ initial alignment angle

f ≡ focal length of optical system

I ≡ transmitted light intensity, signal function

ℓ ≡ reticle line width

r ≡ distance from light spot center

R ≡ light-circle radius

$\rho = \dfrac{2\pi R}{\ell + s}$ ≡ reduced light-circle radius

ρ_o ≡ reduced reticle center-spin center offset

s ≡ reticle line space

$T(x)$ ≡ reticle transmission function

NOMENCLATURE

Θ $\equiv$ angle of gyro rotation

ω_g $\equiv$ gyro angular velocity

ω_{max} $\equiv$ frequency of maximum amplitude of signal spectrum

x , y $\equiv$ light spot center coordinates

x_o $\equiv$ x component of reticle center-spin center offset

I. INTRODUCTION

Satellite Gyro Experiments

Extremely accurate angular measurements are needed in gyro experiments designed to measure relativistic precessions. A number of proposals for such experiments have appeared in recent years[1-5], all with a gyro in orbit around the earth. The precessions to be measured are very small and depend on the gyro and orbital parameters; for a typical earth orbit experiment[1] they are about 3.7×10^{-5} radians/year (for the deSitter Effect) and 2.4×10^{-7} radians/year (for the Lense-Thirring Effect). Note that the inertial frame of the "fixed stars" is known only to a few times 10^{-8} radians/year.

The primary difference between the various proposed experiments has been the system employed to attain readout of the required accuracy. Other considerations, discussed elsewhere[1,6], such as imperfect knowledge of the proper motion of the reference star, gravity gradients, electro-magnetic perturbations, etc., are common to all the proposed experiments and appear to limit accuracy now to a few times 10^{-8} radians/year, of the order of 10% of the Lense-Thirring Effect.

The lower limit on the useful duration of such experiments is set by the inaccuracies in the readout mechanism and possibly from the error in subtraction of stellar aberration. The upper limit is set by satellite durability and/or protection requirements, and by those

backgrounds which grow quadratically in time, e.g. the precession resulting from the earth's gravity gradient acting on the gyro's quadrupole moment in a non-polar orbit. The high accuracy of the autometric gyro readout should make it possible to do useful experiments with durations of only weeks rather than years, thus easing the durability, protection and tending requirements, with a consequent simplification of satellite design.

This paper is a development of a preliminary study[1] of an "autometric readout system, which would combine a very simple but precise and stable physical design with a relatively elaborate mathematical analysis to obtain an extremely high accuracy measurement. Here we present the basis of such an analysis and make error estimates based on available physical components. We conclude that as far as the readout is concerned, an accuracy of about $4 \cdot 10^{-9}$ radians is obtainable.

The Autometric Gyro

As described in Ref. 1, the gyro contains an optical system aligned with its spin axis; the optical system focuses starlight onto a reticle at the back of the gyro (see Fig. 1). Light from a reference star slightly off the optical axis will be focused in the plane of the reticle into an off-center spot which is stationary in a non-rotating frame moving with the gyro center-of-mass. However, in the coordinate frame of the reticle, which rotates with the gyro, the spot runs around a circular path about the spin center. The starlight, interrupted by the reticle pattern, falls on a photomultiplier

behind the reticle and generates a signal dependent upon the reticle configuration and circle radius.

The radius of the circle traced by the spot is directly related to the angle α between the starlight and the gyro axis and the optical system focal length f by

$$R = f \tan \alpha \approx f \alpha \qquad . \qquad (1)$$

Thus determination of the change ΔR of the circle radius R is equivalent to a determination of the angular precession in the starlight-optical axis plane. The difficulty, of course, lies in the smallness of the radius change: for a practical gyro the Lense-Thirring Effect in one year gives only $\Delta R \approx 10^{-5}$ cm, about one-tenth the width of the smallest available reticle lines. But we will find that detailed frequency analysis of the signal can give a usable resolution equivalent to 10^{-7} cm, of the order of 1% of a year's Lense-Thirring Effect and .01% of a year's deSitter Effect for a typical $f \cong 50$ cm.

Since only one parameter is being measured, only one of the two degrees of freedom of the angular precession can be determined. A signal with at least two stars in the field of view is required for the complete determination of the precession. This would require an extension of the analysis given here for the single-star to the two-star case. This does not appear to be difficult although we have not considered it in detail.

A measurement of the precession predicted by theory can be made using only one star provided the initial alignment of the gyro can be set so that the precession is in the starlight-optical axis plane. Fortunately,

a relatively large initial alignment error $\delta\alpha_o$ can be tolerated without a significant decrease in accuracy if the gyro is aimed away from the star in this plane at angle α_o much greater than $\delta\alpha_o$. The fractional error in the precession measurement induced by an initial alignment error angle $\delta\alpha_o$ around α_o will be worst when $\delta\alpha_o$ is out of the plane, being then

$$1 - \cos\left(\frac{\delta\alpha_o}{\alpha_o}\right) \approx \frac{1}{2}\left(\frac{\delta\alpha_o}{\alpha_o}\right)^2 \qquad .$$

Thus, for $\delta\alpha_o = 10^{-4}$ radians, obtainable from a reasonable attitude control system, and $\alpha_o = 10^{-3}$ radians, error from initial alignment would be only 1/2%.

Choice of Reticle and Type of Analysis

The choices of reticle pattern and of type of analysis of the readout signal are closely interrelated: since the tangential velocity of the light spot (as viewed in the gyro reference frame) increases as R increases, the number of reticle line crossings per unit time will increase for a reticle pattern which does not diverge with radius, e.g. a Cartesian grid. Thus time intervals will decrease and spectrum frequencies increase with increasing R. This effect can be enhanced by the use of reticle patterns in which the spacings decrease with increasing radius. However, such patterns necessarily have preferred origins, and it cannot be assumed that these will coincide with the spin center.[6] Indeed, setting the spin axis with such accuracy would require use of a measurement scheme as

accurate as that we are trying to develop.

A way around this difficulty would be to use a special reticle pattern with a preferred origin but to restrict the readout to specified sections of the circumference, a procedure which allows a relatively large error in initial alignment. But analysis of such gated rather than continuous transmission through a reticle with a skew pattern would be intricate, and we have not considered any such case in detail.

We chose the simple linearly ruled reticle (Fig. 2; this is similar to that of Schnopper et al., Ref. 7) along with analysis in the frequency domain because:

1) The signal generated by a linearly ruled reticle is mathematically tractable. Its symmetry properties allow a simple interpretation of grouping the frequency components into odd and even harmonics that enables us to isolate the effects of centering error in the data analysis. In addition to simplicity, the linearly ruled reticle gives very great readout accuracy and easy error compensation. We found that interference effects in the mid-frequency range, caused by the regular periodicity of the linear pattern, provide an extremely sensitive precession indicator. Now that we know how interference effects augment the sensitivity of the linear reticle, we guess that special pattern designs would not give further gain.

2) Non-linear patterns could not be made as fine and as accurate as linear patterns by a grating engine without much technical development. As will be seen later, accuracy increases as both relative error and line spacing decrease--at least for the linear reticle--so the finest pattern obtainable is desired. Line spacings of about 10^{-4} cm are presently available, accurate to 10^{-6} cm.[8]

Outline of Analysis

The gyro output is to be a frequency spectrum generated by electronics in the gyro and/or in an accompanying tender (possibly manned), and possibly telemetered to earth. The arbitrary alignment of, and the imperfections in, the physical construction of the gyro will require several parameters to be matched to the data, giving the reticle center-spin center offset, the mean parameters of the reticle pattern, optical aberrations, etc. In addition, parameters describing the huge periodic effects of stellar aberration on the signal from the gyro in orbit will similarly have to be matched to the data. While we will see that the data could be analyzed completely using only a few frequency components, it would of course pay to overdetermine these parameters as much as possible by using the entire spectrum.

The discussion of analysis will be broken into three parts:

1) "Signal and Spectrum Analysis", the mathematical representation of the signal and its Fourier series.

2) "Utilization", a general program for data analysis.

3) "Error Estimation" for a typical physical system.

II. SIGNAL AND SPECTRUM ANALYSIS

Introductory Analysis of the Signal Function

The reticle coordinates are specified in Fig. 2. The gyro cannot be made accurately enough to specify its spin center in advance, so x_o will be arbitrary. Translational symmetry in the y direction allows us to formally specify $y_o = 0$.

For the gyro rotating with angular velocity ω_g, tracing a circle of light of radius $R = \left((x - x_o)^2 + y^2 \right)^{1/2}$ in the plane of the reticle,

$$x(t) = R \cos \omega_g t + x_o \qquad (2)$$

For a given spot shape the transmitted light intensity, I is a function only of the coordinate x.

$$I \equiv I \left(x[t] \right) = I(R \cos \omega_g t + x_o) \qquad . \qquad (3)$$

This function must be determined from the reticle transmission function $T(x)$ and from the light spot intensity function, $\psi(r)$, where $r = \left((x' - x)^2 + (y' - y)^2 \right)^{1/2}$ is the radius out from the center of the (symmetric) spot. We use only the projection onto the x axis

$$\psi_x(x' - x) = \int_{-\infty}^{+\infty} \psi(x' - x, \, y' - y) \, d(y' - y) \quad \text{(see Appendix)}.$$

The reticle periodicity is the most accurate reference available (as opposed to line widths or spacing), so it will be advantageous

to adjust the reticle parameters to obtain a spectrum with minimal dependence on other factors. This will be the case when $I(x)$ is as close to a sinusoid as possible, and can be accomplished by the use of equal line width ℓ and space s between lines.

We will take $\ell = s$ throughout the rest of this paper, except in the Appendix, where deviations from uniform spacing are specifically considered.

We start our analysis with the approximation of a sinusoidal crossing function:

$$I = \cos \frac{2\pi x}{2\ell} = \cos\left(\frac{\pi}{\ell} [R \cos \omega_g t + x_o]\right) \quad . \quad (4)$$

A complete understanding of the spectrum generated by this simple light intensity function will provide a basis for understanding the spectrum of the actual function. Transforming to dimensionless variables:

$$\rho = \frac{\pi R}{\ell}$$

$$\rho_o = \frac{\pi x_o}{\ell}$$

and $\theta = \omega_g t$, the real angle of rotation, we have

$$I(\theta) = \cos (\rho \cos \theta + \rho_o) \quad (5)$$

Rewriting Eq. (5) as

$$I(\theta) = \cos(\rho \cos \theta) \cos \rho_o - \sin(\rho \cos \theta) \sin \rho_o \quad (6)$$

demonstrates that the Fourier series representation of $I(\theta)$ is expressable as a linear combination of the series representation of $\cos(\rho \cos \theta)$ and $\sin(\rho \cos \theta)$. Both functions are expandable in a cosine series. By considering their behavior under $\theta \to \theta + \pi$, we see that the expansion for $\cos(\rho \cos \theta)$ contains only even terms while that for $\sin(\rho \cos \theta)$ contains only odd terms. This property greatly simplifies the analysis since it allows us to isolate the effects of x_o. This reflects a basic symmetry property of the reticle pattern. Referring to Fig. 2, we see that there are two equivalent definitions of the reticle origin. A reticle rotating about the center of a space--e.g. $x_o = 0$ in Fig. 2-- or about the center of a line, e.g. $x_o = \ell$, has $\rho_o = n\pi$, where n is integral, and will generate only even components of the spectrum. A reticle centered on the boundary between a space and a line, e.g. $x_o = \frac{\ell}{2}$ in Fig. 2, has $\rho_o = (n + 1/2) \pi$ and will generate only odd components. The case of any off-center reticle with neither of these choices of ρ_o is reducible to a superposition of the two on-center cases. Effectively there are two separate channels, each containing enough information to determine the light circle radius exactly. Separate determination of the precession can be made from each channel and the mean used for the most probable result.

The Spectrum and Its Qualitative Analysis

Fig. 3 presents the numerically generated spectrum of $I(\theta)$ for a typical R and arbitrary x_o. The complete spectrum and even and odd component series are plotted separately for comparison. Fig. 4 presents plots of the odd component series for $\Delta R = 0.12\ell$ and $\Delta R = 0.24\ell$. These correspond

to precessions of 2.4×10^{-7} and 4.8×10^{-7} radians, the predicted Lense-Thirring precessions for one and two years or the predicted deSitter precessions for 24 and 48 days. The most noticeable change is the drastic amplitude change in the region about $270\ \omega_g\ (\approx \rho\omega_g/\sqrt{2})$.

The amplitude of the nth spectrum component is given by the Fourier cosine coefficient $a_n(\rho)$

$$a_n(\rho) = \frac{1}{\pi} \int_0^{2\pi} I(\theta)\cos n\theta\ d\theta \qquad . \qquad (7)$$

To understand the spectrum character qualitatively it is convenient to consider the terms in Eq. (6) separately. That is, $I(\theta) = \cos(\rho\cos\theta)$ or $I(\theta) = \sin(\rho\cos\theta)$. The same arguments hold for both functions which, as mentioned, correspond to the even and odd component series.

Since $I(\theta)$ is a rapidly oscillating function (there are about 240 cycles in the range $0 < \theta < 2\pi$ for the $\rho \approx 380$ we are using in this example), it is reasonable to assume almost complete cancellation of those portions of the integrals in which the instantaneous frequency does not equal the component frequency $n\omega_g$. Thus, to a good approximation, the magnitude of any component will be determined strictly by the specific regions of $I(\theta)$ where the instantaneous frequency $\approx n\omega_g$. Physically we see that each spectrum frequency component is associated with specific generating regions on the reticle. The instantaneous frequency associated with the region about θ for this reticle is $\frac{d(\rho\cos\theta)}{dt} = -\rho\omega_g \sin\theta$.

The signal is strongest in the high frequency range because of the comparatively large fraction of the time the spot is moving almost normal to the lines. Thus we expect an overall increase of spectrum

intensity with frequency until the frequency

$$\omega_{max} = \frac{\pi R}{\ell}\, \omega_g = \rho\omega_g \qquad (8)$$

is reached at $\theta = \frac{\pi}{2}$. Actually, the spectrum peak for non-zero spot and line widths is at a slightly lower frequency.

Because of the up-down symmetry of the reticle, and its right-left symmetry (anti-symmetry) for $x_o = 0$ $(\frac{\ell}{2})$, there are four strong generating regions for each frequency, one in each quadrant of the reticle. These degenerate to the two regions of normal crossing at the maximum frequency. The peaks and dips in the frequency spectrum are caused by interference between these four regions; the frequency dependence of their relative phase determines the fine structure within the spectrum envelope.

We do not know how to describe in the time domain just how the motion of the spot controls the neatness of the interference pattern in different regions of the frequency spectrum. However, it does seem reasonable that the regions corresponding to the simple angles $\theta = \pi/2$, $\pi/4$, $\pi/6$ and $\pi/8$ are particularly neat, as is conspicuous in the spectra in Fig. 3.

On the other hand, the origin of these regions is simply understood in the frequency domain. They appear when the period of the interference pattern is a simple fractional multiple of the difference between the frequency components, in a manner analogous to stroboscopic observation or periodic motion.[9]

Full Analysis of Sinusoidal Crossing Function

Instead of evaluating Eq. (7) directly we use Jacobi's results:

$$\cos(\rho \cos \theta) = J_0(\rho) + 2 \sum_{n=1}^{\infty} (-1)^n J_{2n}(\rho) \cos 2n\theta \qquad (10)$$

$$\sin(\rho \cos \theta) = 2 \sum_{n=1}^{\infty} (-1)^{n+1} J_{2n-1}(\rho) \cos(2n - 1) \theta \quad . \qquad (11)$$

We can identify the coefficients of $\cos 2n\theta$ and $\cos(2n - 1)\theta$ with the $a_n(\rho)$.

Removing the uniform multiplicative constant $\frac{2}{\pi}$ we have,

$$a_n(\rho) = \begin{cases} (-1)^{\frac{n-1}{2}} \sin \rho_0 \, J_n(\rho) \quad , \; n \text{ odd} & (12) \\ (-1)^{\frac{n}{2}} \cos \rho_0 \, J_n(\rho) \quad , \; n \text{ even} & (13) \end{cases}$$

Fig. 5 is a graph of $J_\eta(\rho)$ as a function of η, where η varies continuously. The even component spectrum displayed in Fig. 3 is obtainable from this curve by taking the absolute value and drawing straight lines between points where the plot crosses even integral values of η. A similar procedure at the odd points generates the odd component spectrum. Of course, both spectra must be scaled by the appropriate factors, $\cos \rho_0$ and $\sin \rho_0$ respectively. Explicit representations of the regularities in the spectrum envelope and their dependence on ρ can be obtained by expanding $a_n(\rho)$ about the regular points (e.g. $\frac{\sqrt{2}}{2} \rho \omega_g$). This process and the resultant formulae are described elsewhere.[9]

Analysis with Arbitrary Crossing Function

Since it is periodic in x, the signal function can be expressed in a Fourier series:

$$I(x) = \sum_{m=0}^{\infty} (a_m^x \cos mx + b_m^x \sin mx) \tag{14}$$

where the a_m^x, b_m^x are the Fourier coefficients of I as a function of x (see Appendix) giving

$$I(\theta) = \sum_{m=0}^{\infty} a_m^x \cos m(\rho \cos \theta + \rho_o) + b_m^x \sin m(\rho \cos \theta + \rho_o) \tag{15}$$

$$= \sum_{m=0}^{\infty} (a_m^x \cos m\rho_o + b_m^x \sin m\rho_o) \cos(m\rho \cos \theta)$$

$$+ \sum_{m=1}^{\infty} (-a_m^x \sin m\rho_o + b_m^x \cos m\rho_o) \sin(m\rho \cos \theta) \tag{16}$$

Thus, the Fourier series of $I(\theta)$ can be represented as a superposition of the Fourier series of the basic signal functions $\cos(m\rho \cos \theta)$, $\sin(m\rho \cos \theta)$. The components corresponding to the first part of Eq. (16) are all even multiples of ω_g while those corresponding to the second part are all odd multiples. The determination of the a_m^x, b_m^x allows us to separate the experimental spectrum into sinusoidal crossing function spectra corresponding to multiples of ρ which are then used for precession determination. These coefficients can be obtained by solution of a system of linear equations using the spectrum component magnitudes as the known variables. This procedure is simplified by

three facts:

1) As seen in Figs. 3 and 4, the components of $\cos(\rho \cos \theta)$, $\sin(\rho \cos \theta)$ quickly become negligible above $\omega = \rho\omega_g$. However, the primary range of the mth terms in Eq. (16) extends to $m\rho\omega_g$ so the coefficients can be progressively determined by starting in the high frequency region and working down.

2) In actuality, only two or three of the coefficients will be significant.

3) $I(\theta)$ can still be completely expanded in a cosine series so the relative component phases will be defined to an easily resolved 180° ambiguity.

Figure 6 is the odd component spectrum from a computer simulation of a typical crossing function; only the primary range is shown. As can be seen by comparison with Fig. 3, the differences are not large and do not mask the essential structures.

III. UTILIZATION

In determining gyro precession from relative changes in the
spectrum components we should try to isolate that part of the data which
is dependent on only the reticle periodicity. This is automatically done
by the initial separation of the spectrum into sinusoidal crossing function
spectra whose structure is dependent solely on the reticle periodicity.
All further analysis involves these separated spectra.

While ρ could be determined by a least square fit of Eqs. (12,
13) a more accurate procedure would be to emphasize the regions of the
spectrum with greater than average sensitivity. This is done by using
the peak region of the spectrum for a coarse reading of ρ and then using
the interference region for a very accurate reading of ρ and thence R.

The Spectrum Peak

ρ can be determined from the spectrum peak position ω_{max} by
Meissel's relation:[9]

$$\omega_{max} = 2\pi \left(\rho - .8086\rho^{1/3} + \ldots\right) \quad . \tag{17}$$

Since ω_{max} need not be an integer, its value must be interpolated from
the surrounding spectrum components. This interpolation is not difficult
since the form of the spectrum is known (see Ref. 9, Appendix H). Even an
interpolation accuracy of only half the difference between the components

determines ρ to a fractional accuracy of $\frac{1}{2\rho}$. This gives $\Delta\omega_{max}/\omega_{max} \approx$ $2 \cdot 10^{-3}$ for $\rho \sim 400$, a typical value, more than accurate enough for use as an initial coarse reading.

The Interference Region

The amplitudes in the interference region have sensitivities of the order of 100% for a unit change in ρ independent of the initial value of ρ (see Ref. 9, Appendix E). Thus readout sensitivity from this region is essentially independent of the initial alignment angle α_o.

Use of the change in magnitude of any component, $\Delta|a_n(\rho)|$, as a precession indicator requires knowledge of $\frac{d|a_n(\rho)|}{d\rho}$. This derivative may be calculated directly from the observed spectrum by the Bessel function recurrence relation:

$$\rho \frac{\partial J_\eta(\rho)}{\partial\rho} + \rho J_\eta(\rho) = \eta J_{\eta-1}(\rho) \quad . \tag{18}$$

As seen from the formula, determination of the derivatives of either the odd or even component series requires use of the alternate series. This requires accurate normalization of the series relative to each other.

An alternate method is to utilize our knowledge of the form of the spectrum to determine the derivatives indirectly. Since we are con- sidering components in the intermediate spectrum region, we may use Rayleigh's approximation for $J_\eta(\rho)$ in Eqs. (12,13) resulting in:

$$a_n(\rho) = \begin{cases} \sin \rho_0 \dfrac{\sin \varphi(n,\rho)}{(\rho^2 - n^2)^{1/4}} & , \text{ n odd} \qquad (19) \\[4mm] \cos \rho_0 \dfrac{\cos \varphi(n,\rho)}{(\rho^2 - n^2)^{1/4}} & , \text{ n even} \qquad (20) \end{cases}$$

where $\varphi(n,\rho) = \sqrt{\rho^2 - n^2} + n \sin^{-1}\left(\dfrac{n}{\rho}\right) - \dfrac{\pi}{4}$.

A crude determination of ρ from the spectrum peak will enable us to normalize the spectrum components and remove the denominators of Eqs. (19,20). This isolates the rapidly varying part of the spectrum $a_n^r(\rho)$.

$$a_n^r(\rho) = \begin{cases} \sin \varphi(n,\rho) & , \text{ n odd} \qquad (21) \\[3mm] \cos \varphi(n,\rho) & , \text{ n even} \qquad (22) \end{cases}$$

from which we obtain

$$\frac{\partial a_n^r(\rho)}{\partial \rho} = \begin{cases} \cos \varphi(n,\rho) \dfrac{\partial \varphi}{\partial \rho} & , \text{ n odd} \qquad (23) \\[4mm] -\sin \varphi(n,\rho) \dfrac{\partial \varphi}{\partial \rho} & , \text{ n even} \qquad (24) \end{cases}$$

$$\frac{\partial \varphi}{\partial \rho} = \sqrt{1 - \left(\frac{n}{\rho}\right)^2} \qquad \qquad (25)$$

The fractional change in normalized component intensities is given by

$$\frac{\dfrac{\partial a_n^r(\rho)}{\partial \rho}}{a_n^r(\rho)} = \begin{cases} \cot \varphi(n,\rho) & , \text{ n odd} \qquad (26) \\[3mm] -\tan \varphi(n,\rho) & , \text{ n even} \qquad (27) \end{cases}$$

These equations indicate that component magnitudes change from maxima to minima for $\Delta\varphi = \frac{\pi}{2}$. For "typical" gyro parameters ($f = 50$ cm, line spacing $= 10^{-4}$ cm) this corresponds to $\Delta\alpha = 6.8 \times 10^{-7}$ radians, the Lense-Thirring precession in 2.8 years.

As can be seen from Eqs.(26, 27) fractional precession sensitivity becomes arbitrarily large for component magnitudes approaching zero. A lower limit on usable component magnitudes will be set by the absolute noise level of the system, to be discussed in the next section.

IV. ERROR ANALYSIS

The main sources of readout error are expected to be (1) the reticle, (2) the optical system, (3) photon noise, and (4) mechanical and thermal changes of the gyro in operation. No consideration of mechanical and thermal problems has been given beyond the small amount in Refs. 6 and 9; they are expected to be controllable but need detailed planning.

Reticle

The previous analysis incorporates all reticle characteristics that can be represented by one dimensional Fourier series (e.g., the reticle line cross-sections). However, periodic and random error in line spacing is expected to have a magnitude $\epsilon_\ell \approx 10^{-6}$ inches.[8] Computer simulation indicates that these errors will create a fairly uniform spectrum of background noise over the frequency region of interest, giving for a reticle having 10^4 lines/cm a noise intensity to spectrum envelope ratio of about .01 which agrees with the predicted noise ratio $\frac{\epsilon_s}{2\ell}$. These intensity errors induce a fixed rather than fractional error in precession determination. This error is computed from Eqs. (23,24), evaluated at $a_n^r(\rho) \approx 0$ since typically the minimal components will be used for the final measurements, giving

$$\Delta\rho = \frac{\Delta a_n^r(\rho)}{\frac{\partial \varphi(n,\rho)}{\partial \rho}} \approx \Delta a_n^r(\rho) = \frac{\epsilon_s}{2\ell} \approx .01$$

where n is a null component.

This corresponds for $\ell = 10^{-4}$ cm to

$$\Delta R = \frac{(2\ell)}{2\pi} \Delta\rho = \frac{\epsilon_\ell}{2\pi} \approx 10^{-7} \text{ cm}$$

and (f = 50 cm)

$$\Delta\alpha \approx 2 \times 10^{-9} \text{ radians}$$

To be conservative in design we double this figure and estimate

$$\Delta\alpha = 4 \times 10^{-9} \text{ radians}$$

Optical System

Optical system defects can cause aberrations in both the light spot shape and the path traced out on the reticle.

The exact form of the light spot intensity function is in principle unimportant since, as with the reticle line cross sections, the required information can be determined from the spectrum itself. Circular symmetry is required for the crossing function to remain dependent solely on the x coordinate but this is not expected to be a problem in such paraxial optics.

Angular misalignments between the optical axis, gyro spin axis, and reticle normal are expected to be about 10^{-5} radians each. Errors from these will be negligible since we are working in the paraxial region.

Photon Noise

In order for the photon shot noise to be fractionally small enough to measure $2 \cdot 10^{-9}$ radians using the light from e.g. Mintaka (δ-Orionis) with an optical aperture of e.g. 20 cm radius, an exposure time of about a second is necessary. The real time available is severely limited, however, because the stellar aberration from the gyro's orbital motion gives a huge sinusoidal background modulation, swinging $\pm 10^{-4}$ radians with a period of only about $6 \cdot 10^{3}$ seconds. Intervals of the order of 10 seconds in which α should be stationary to 10^{-9} radians are available near the peaks of this orbital modulation. Thus in about an hour we can in principle get one good measurement on all component frequencies without being limited by photon noise.

V. SUMMARY

A simple reticle with parallel equally spaced lines to transmit light in an autometric gyro is shown to give a signal which can be used for very accurate angular precession measurements. Frequency analysis of the signal is chosen over time domain analysis and/or over a specially designed reticle.

Gyro precession will induce a change in the interference structure of the spectrum in addition to dilating the overall frequency distribution. The expected output spectrum has been analytically determined, exhibiting the dependence on spot and reticle line cross sections and line spacing so that they can be precisely determined from the output data.

The spectrum structure is extremely sensitive to precession. Computer simulations indicate that accuracy will be limited by reticle line spacing variations to $\pm 4 \cdot 10^{-9}$ radians. This would allow a Lense-Thirring precession measurement accurate to $\pm 20\%$ in 30 days (accuracy being limited by physical effects common to all such experiments) or a $\pm 1\%$ deSitter precession measurement in four days.

ACKNOWLEDGEMENTS

APPENDIX

The Crossing Function

The signal function $I(x)$ can be determined by numerical integration of the light spot intensity function $\psi_x(x' - x)$ over the reticle transmission function $T(x')$:

$$I(x) = \int_{-\infty}^{\infty} T(x') \, \psi_x(x' - x) \, dx' \tag{28}$$

where we have assumed that the reticle is virtually infinite.

Since $I(x)$ is periodic, it can be expressed in a Fourier series. The period is the reticle line width ℓ plus gap space s.

For reticle lines with symmetric opacity about their centers and $\ell = s$, the transmission function $T(x)$ has the symmetry properties

$$T(x) = T(-x) \tag{29}$$

$$T(\ell - x) = -T(x) \quad . \tag{30}$$

For manipulative convenience the crossing function has been chosen to vary between -1 and +1 rather than between 0 and 1.

These equations imply that the crossing function can be expanded by the restricted series

$$I(x) = \sum_{m \text{ odd}} a_m^x \cos \frac{\pi}{\ell} x \tag{31}$$

Fortunately, only the first few terms of the expansion are required in practice. Numerical results, obtained with a diffraction-limited spot $(J_1(\zeta)/\zeta)^2$ (where $\zeta = \frac{Dr}{\lambda f}$, D is the mirror diameter, f its focal length, λ is the reduced wavelength of the starlight, and r the distance from the spot center) falling on a perfect reticle, showed that one term in the sinusoidal approximation gave agreement to 10% and two terms to 0.5%.

The symmetry properties of Eqs. (29,30) are expected to be violated by about 2% because of asymmetry of the opacity of the reticle lines about their centers and inequality between line width and gap width in an actual reticle. These deviations will be the same for each line so $T(x)$ remains periodic. However, Eq. (31) is no longer exact. In practice, only a few additional terms would be required. We have not gone into these questions, except to note that in studying the crossing function from a periodic reticle with asymmetric lines and with an arbitrary light spot intensity function, it will be convenient to isolate the effects of variation in $T(x)$ and $\psi_x(x)$ by representing the Fourier coefficients of $I(x)$ (a_m^X , b_m^X) as functions of the coefficients of $T(x)$ (a_m^T , b_m^T) and the Fourier cosine and sine transforms $[a^\psi(p) , b^\psi(p)]$ of $\psi_x(x)$. A simple derivation similar to the convolution theorem of Fourier analysis gives:

$$a_m^X = a_m^T\, a^\psi(km) + b_m^T\, b^\psi(km) \tag{32}$$

$$b_m^X = -a_m^T\, b^\psi(km) + b_m^T\, a^\psi(km) \tag{33}$$

where $k = \frac{2\pi}{\ell + s}$.

For a circularly symmetric light spot, $b^\psi(km) \equiv 0$.

FIGURE CAPTIONS

Fig. 1   Gyro and Photomultiplier. Note that the lens system shown is only schematic; a Cassegranian mirror system with the reticle at the center of the large mirror might be preferable.

Fig. 2   Reticle Coordinates. The dotted circle represents the fuzzy boundary of the circular light spot, and the solid circle shows the path traced out by its center. For the cases studied the path swept across some one hundred and twenty solid lines, i.e. $R \approx 60(l + s) = 120l$.

Fig. 3   The Signal Spectrum Using a Sinusoidal Crossing Function. While the actual spectrum is discrete, a continuous line is used in this and other spectrum plots for graphical and interpretative ease. Only the values at the relevant (even or odd or both) integral arguments are significant. The magnitude of the amplitude--i.e. the square root of the intensity--is plotted, since it is not intended to measure phases. The scale of amplitude is relative. The abscissa is angular frequency in terms of the gyro angular frequency ω_g. In Figure 3a all components are plotted. Figures 3b and 3c show only even and odd components. A radius R and an x-coordinate of the center, x_o, were chosen at random, giving $R = 121.371l$ (hence $\rho = \pi R = 381.30$) and $x_o = .32l$, where l is

Fig. 3
(Cont'd)
the line width which here equals the gap space s).

Fig. 4   Spectrum Variation with Precession Using a Sinusoidal

Crossing Function; Odd Components only. A year of Lense-

Thirring (or 24 days of deSitter) precession changes Fig. 4a

to Fig. 4b, with a radius change $\Delta R = .12\ell$. After two years

we have Fig. 4c, with $\Delta R = .24\ell$. Some regions of the spectrum

of exceptional neatness are marked in Fig. 4a and labeled with

the value of θ for the corresponding generating region of the

light path on the reticle.

Fig. 5   High Order Bessel Function with a Fixed Argument: $J_\eta(381.30)$.
The abscissa is the order η.

Fig. 6   Spectrum from Realistic Crossing Function. The odd components

of the spectrum using the crossing function from a diffraction-

limited spot of diameter approximately equal to ℓ. The quan-

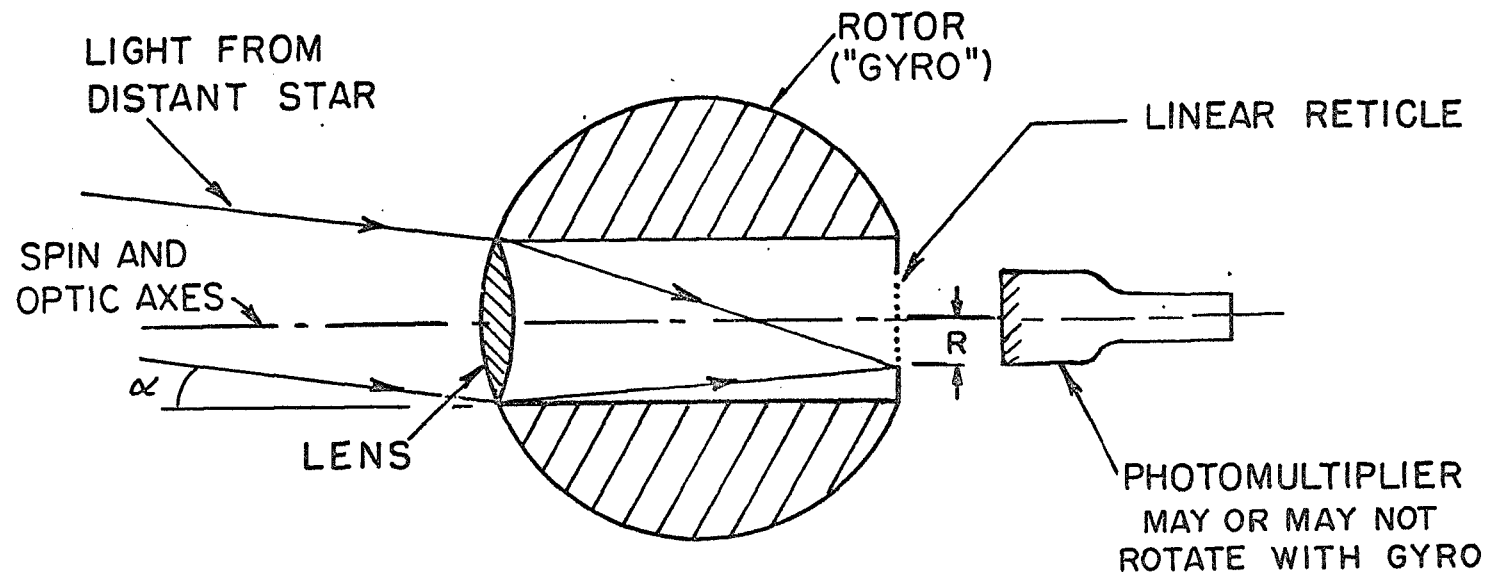tities R and x_o are the same as in Figs. 3 and 4a.

LIGHT FROM
DISTANT STAR

SPIN AND
OPTIC AXES

α

LENS

ROTOR
("GYRO")

LINEAR RETICLE

R

PHOTOMULTIPLIER
MAY OR MAY NOT
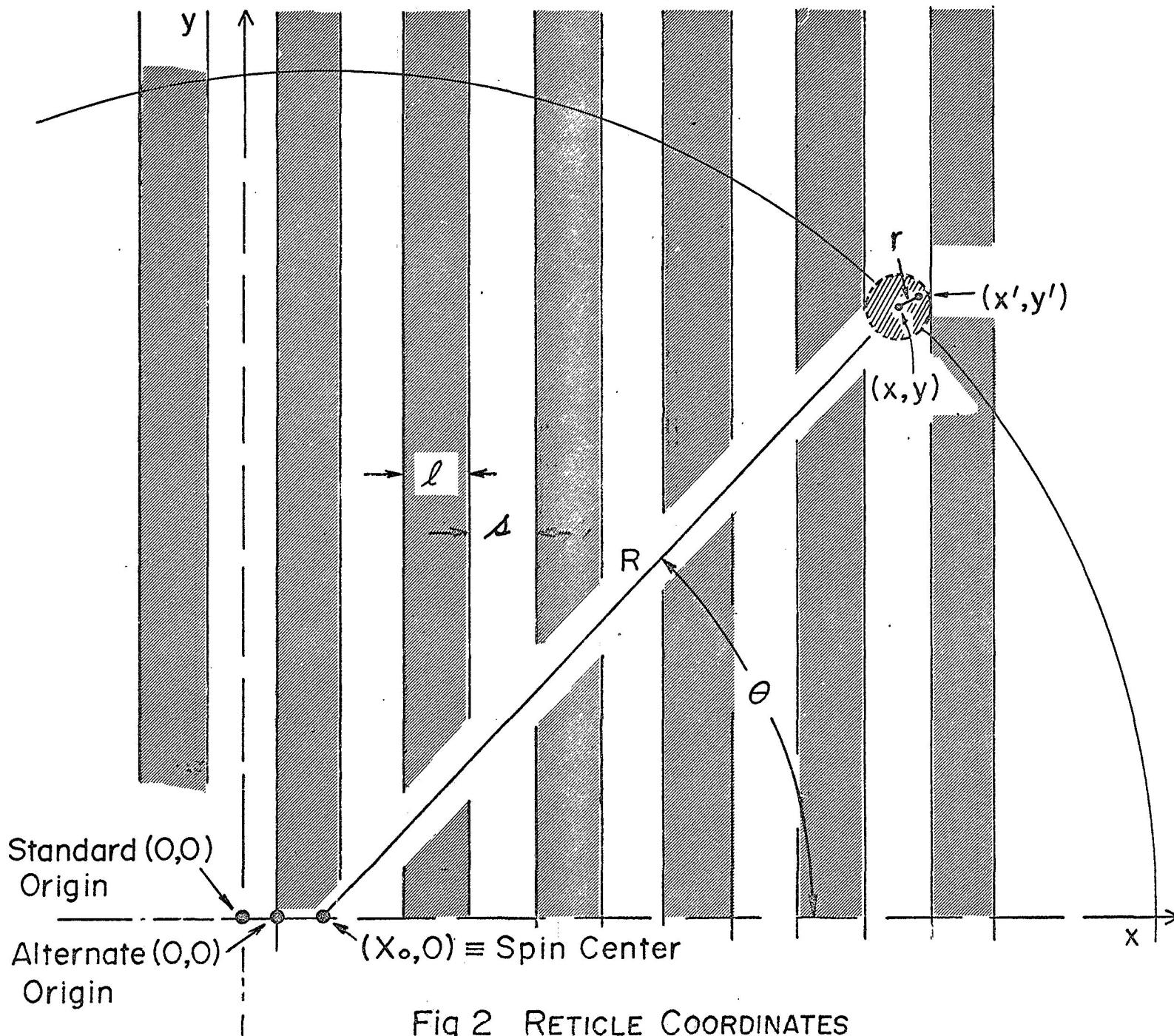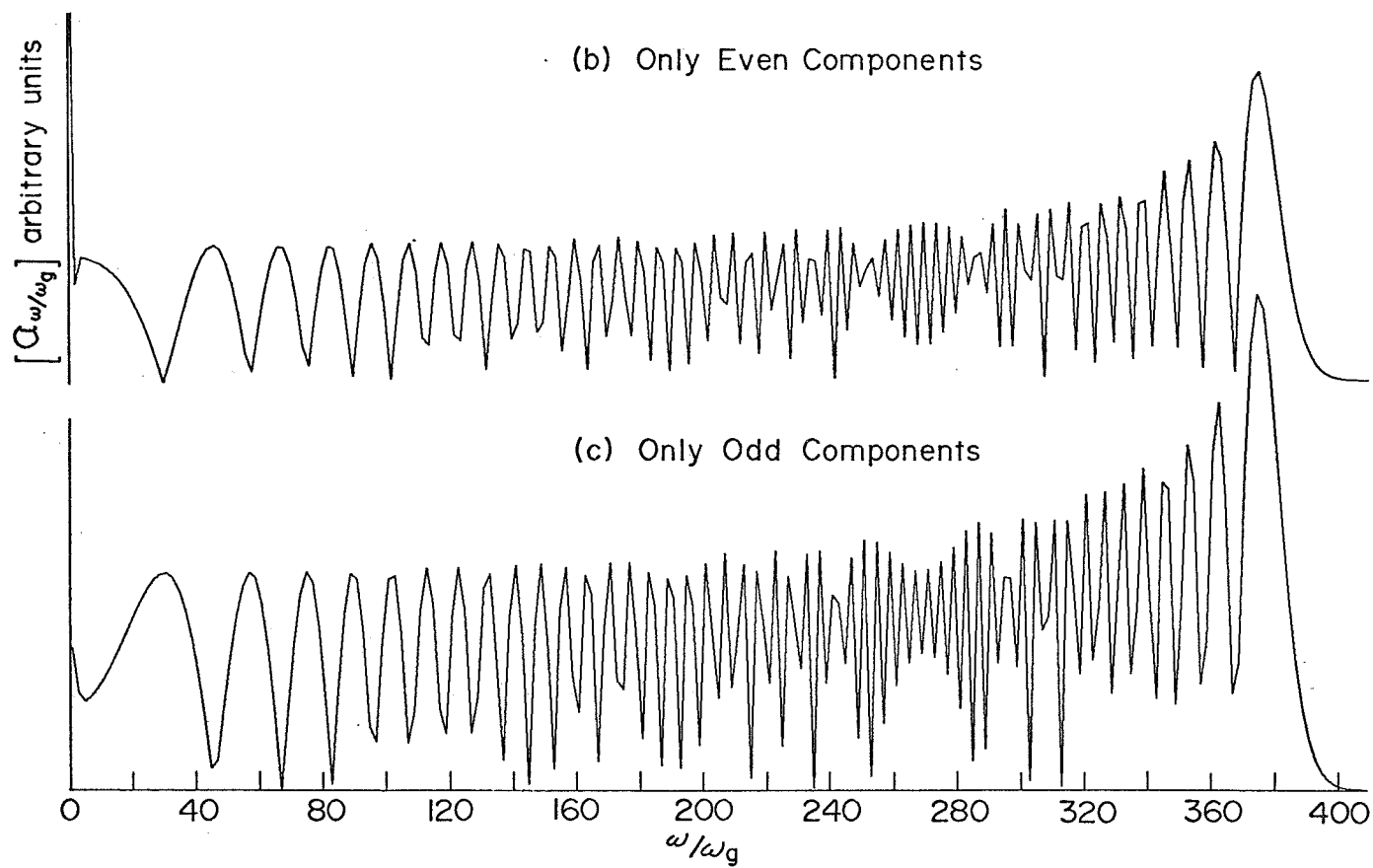ROTATE WITH GYRO

Fig. 1 GYRO AND PHOTOMULTIPLIER

32

Fig 2 RETICLE COORDINATES

33

Fig. 3
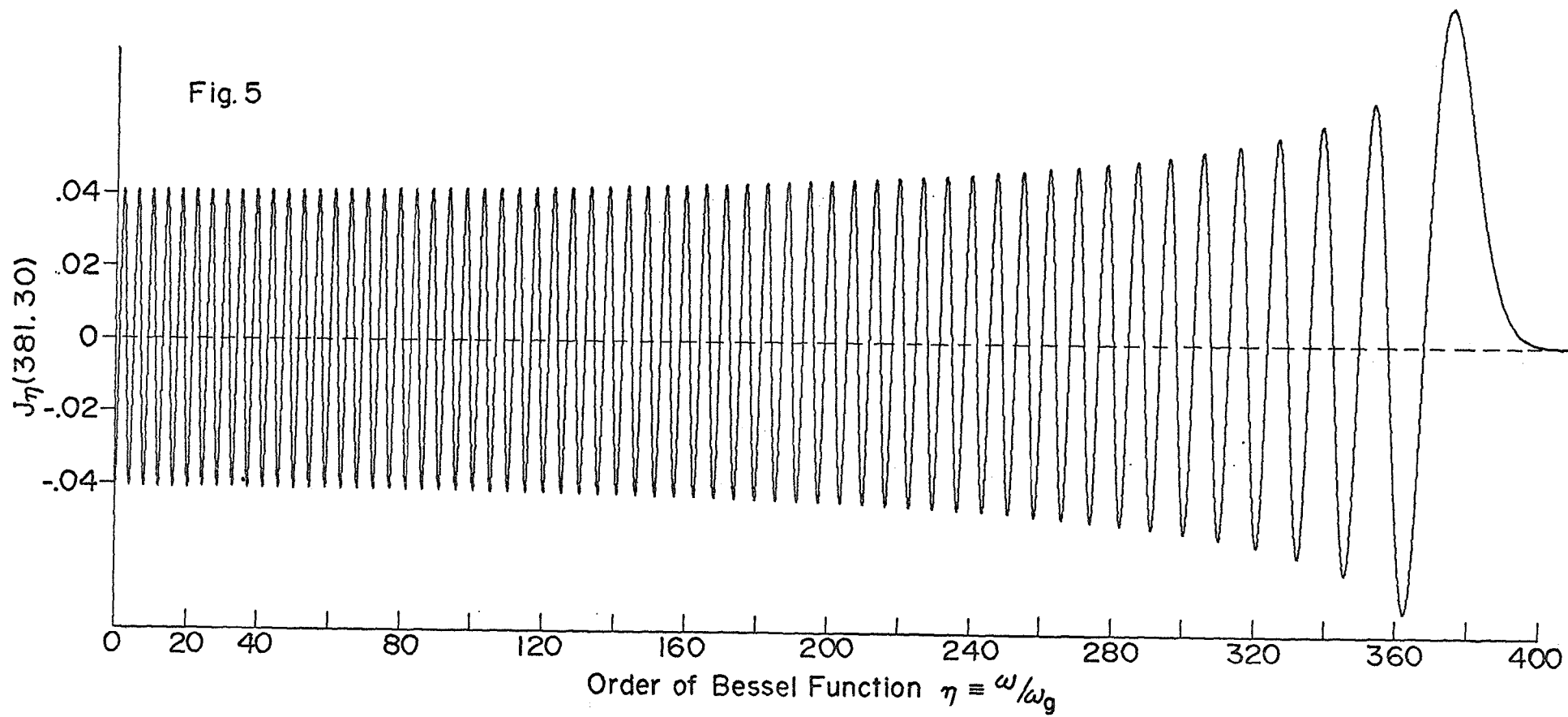
(a) All Components

$R = 121.371 \ell$

$x_o = 0.32 \ell$

(b) Only Even Components

$[a_{\omega/\omega_g}]$ arbitrary units

(c) Only Odd Components

ω/ω_g

Fig. 4

(a) t = 0

$R = 121.371 \ell$
$x_o = 0.32 \ell$

$\theta = \pi/4$ i.e.
$\omega/\omega_g \sim \frac{\rho}{\sqrt{2}}$

$\theta = \pi/8$ $\theta = \pi/6$

(b) t = 1 year

$R = 121.491 \ell$
$x_o = 0.32 \ell$

(c) t = 2 years

$R = 121.611 \ell$
$x_o = 0.32 \ell$

$[a_{\omega/\omega_g}]$ arbitrary units

ω/ω_g

Q   40   80   120   160   200   240   280   320   360   400

Fig. 5

$J_\eta(381.30)$

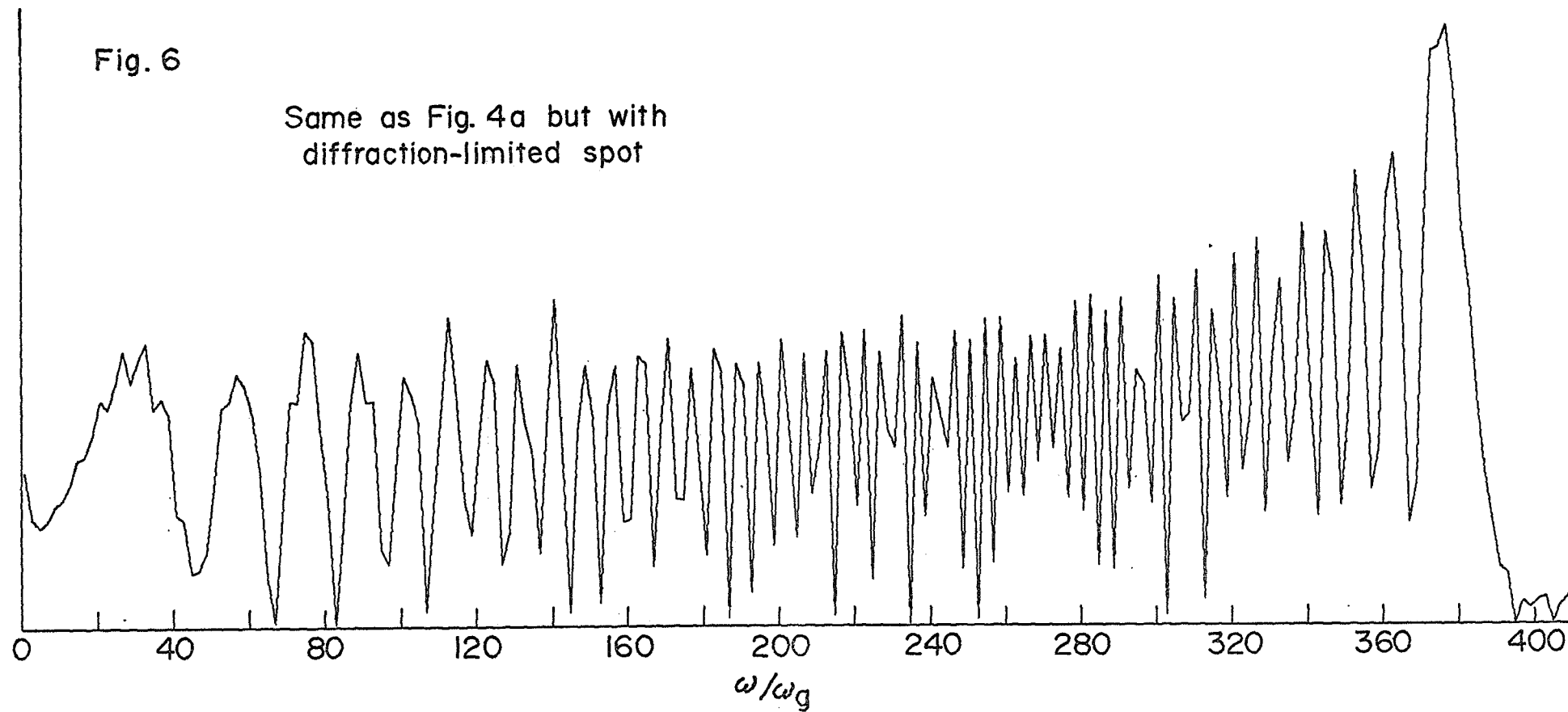Order of Bessel Function $\eta \equiv \omega/\omega_g$
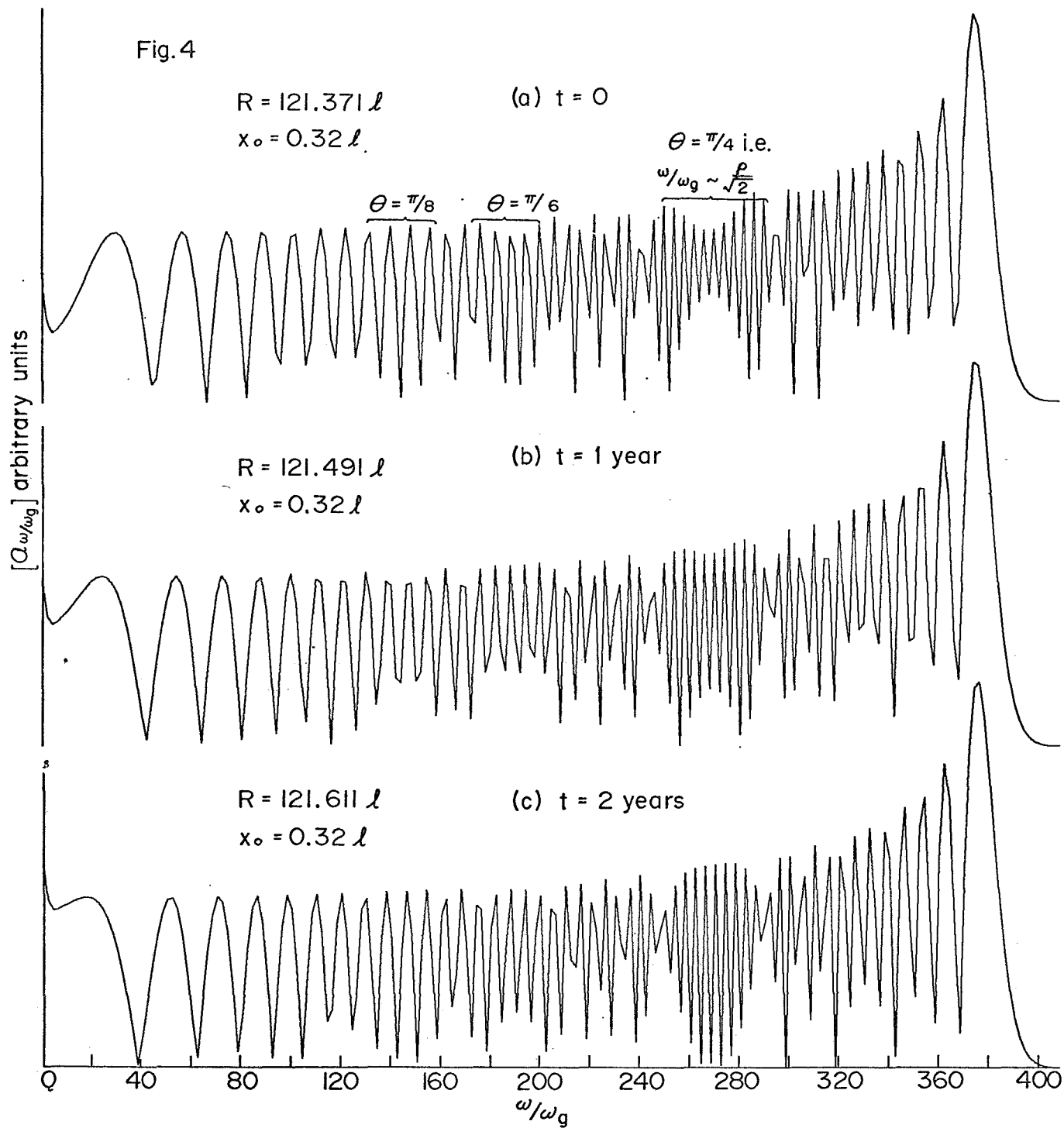
Fig. 6

Same as Fig. 4a but with
diffraction-limited spot

ω/ω_g

37

REFERENCES

1.   D. H. Frisch and J. F. Kasper, Jr.,   J. App. Phys., Vol. 40, 8, 3376, (1969).

2.   R. Palamara, AIAA J., 4, 1036 (1966).

3.   H. W. Knoebel, W. D. Compton, "Research Related to an Experimental Test of General Relativity," Coordinated Science Lab, University of Illinois, (1966).

4.   W. Fairbank and C. Everitt, "Application of Low Temperature Techniques to a Satellite Test of General Relativity," unpublished report, Dept. of Physics, Stanford University, (1967).

5.   B. Lange, Proceedings 1963 Conference on Unconventional Inertial Sensors, (Farmingdale, L. I., New York, 1963).

6.   J. F. Kasper, Jr., "A Feasibility Study of an Orbital General Relativity Experiment," unpublished Sc.D. thesis, Dept. of Aeronautics and Astronautics, Massachusetts Institute of Technology, (1968).

7.   H. W. Schnopper, R. I. Thompson, and S. Watt, Space Sci. Rev., 8, 534, (1968).

8.   G. W. Stroke, Progress in Optics, Vol. II, (E. Wolf, ed.), New York: John Wiley and Sons, (1963), and G. Harrison, personal communication.

9.   D. I. Shalloway, "Read-out Analysis for an Autometric Gyro," unpublished S.B. thesis, Dept. of Physics, Massachusetts Institute of Technology (1969).